Research report

TDCS increases cortical excitability: Direct evidence from TMS–EEG

Leonor J. Romero Lauro [a,], Mario Rosanova [b,c], Giulia Mattavelli [a], Silvia Convento [a], Alberto Pisoni [a], Alexander Opitz [d], Nadia Bolognini [a,e] and Giuseppe Vallar [a,e]*

[a] *Department of Psychology, University of Milano-Bicocca, P.za Ateneo Nuovo 1, Milano, Italy*
[b] *Department of Biomedical and Clinical Sciences "L. Sacco", University of Milano, Via GB Grassi 74, Milano, Italy*
[c] *Fondazione Europea di Ricerca Biomedica FERB Onlus, Milano, Italy*
[d] *Department of Clinical Neurophysiology, Robert-Koch-Straße 40, Göttingen, Germany*
[e] *Laboratory of Neuropsychology, IRCCS Istituto Auxologico Italiano, Via Mercalli 32, Milano, Italy*

ARTICLE INFO

ABSTRACT

Despite transcranial direct current stimulation (tDCS) is increasingly used in experimental and clinical settings, its precise mechanisms of action remain largely unknown. At a neuronal level, tDCS modulates the resting membrane potential in a polarity-dependent fashion: anodal stimulation increases cortical excitability in the stimulated region, while cathodal decreases it. So far, the neurophysiological underpinnings of the immediate and delayed effects of tDCS, and to what extent the stimulation of a given cerebral region may affect the activity of anatomically connected regions, remain unclear. In the present study, we used a combination of Transcranial Magnetic Stimulation (TMS) and Electroencephalography (EEG) in order to explore local and global cortical excitability modulation during and after active and sham tDCS. Single pulse TMS was delivered over the left posterior parietal cortex (PPC), before, during, and after 15 min of tDCS over the right PPC, while EEG was recorded from 60 channels.

For each session, indexes of global and local cerebral excitability were obtained, computed as global and local mean field power (Global Mean Field Power, GMFP and Local Mean Field Power, LMFP) on mean TMS-evoked potentials (TEPs) for three temporal windows: 0–50, 50–100, and 100–150 msec. The global index was computed on all 60 channels. The local indexes were computed in six clusters of electrodes: left and right in frontal, parietal and temporal regions.

GMFP increased, compared to baseline, both during and after active tDCS in the 0–100 msec temporal window. LMFP increased after the end of stimulation in parietal and frontal clusters bilaterally, while no difference was found in the temporal clusters. In sum, a diffuse rise of cortical excitability occurred, both during and after

* *Corresponding author.* Department of Psychology, University of Milano-Bicocca, Piazza Ateneo Nuovo, 1, 20126 Milano, Italy.
E-mail addresses: leonor.romero1@unimib.it, l.romerolauro@gmail.com (L.J. Romero Lauro).

active tDCS. This evidence highlights the spreading of the effects of anodal tDCS over remote cortical regions of stimulated and contralateral hemispheres.

1.   Introduction

Transcranial direct current stimulation (tDCS) is offering new perspectives in cognitive neuroscience and neuropsychology in both research and therapeutic settings. Several studies have successfully employed tDCS to modulate cortical excitability, in turn affecting a wide range of sensorimotor and cognitive functions in healthy and pathological human brains (see Antal, Paulus, & Nitsche, 2011; Jacobson, Koslowsky, & Lavidor, 2012; Nitsche & Paulus, 2011; Utz, Dimova, Oppenlander, & Kerkhoff, 2010; Vallar & Bolognini, 2011 for reviews). This evidence has fostered the application of this technique in rehabilitation settings (e.g., Brunoni et al., 2011), based on results showing that tDCS may induce not only on-line effects on spontaneous neuronal activity, but also long-lasting after-effects likely mediated by mechanisms of synaptic long-term potentiation and depression (i.e., LTP and Long-term Depression, LTD, respectively), which affect neuroplasticity (Liebetanz, Nitsche, Tergau, & Paulus, 2002; Nitsche, Fricke et al., 2003, 2008; Stagg et al., 2009).

tDCS is effective in the rehabilitation of patients with neuropsychiatric and neurological disorders such as epilepsy (Fregni, Thome-Souza et al., 2006; Nitsche & Paulus, 2009), Parkinson's (Fregni et al., 2006) and Alzheimer's disease (Ferrucci et al., 2008), chronic pain (O'Connell et al., 2011; Bolognini, Olgiati, Maravita, Ferraro, & Fregni, 2013), migraine (Antal et al., 2008; Dasilva et al., 2012), major depression (Boggio et al., 2008; Ferrucci et al., 2009; Brunoni et al., 2011; Nitsche, Boggio, Fregni, & Pascual-Leone, 2009), as well as cognitive and motor disorders of patients with cerebrovascular diseases (Bolognini, Pascual-Leone, & Fregni, 2009; Gomez et al., 2013; Kandel, Beis, Le Chapelain, Guesdon, & Paysant, 2012; Monti et al., 2012; Mylius et al., 2012).

tDCS offers several advantages that render this tool so attractive for neuro-rehabilitation, as compared with other brain stimulation techniques: it is safer than invasive brain stimulation, which is usually associated to higher surgical risks and costs; in comparison to Transcranial Magnetic Stimulation (i.e., TMS), it is less uncomfortable, easier to handle and less expensive.

Despite being increasingly used, the precise neurophysiologic mechanisms underlying tDCS effects remain to be fully elucidated. At a neuronal level, tDCS modulates cortical excitability by shifting the resting membrane potential in a polarity-dependent way: anodal stimulation increases the spontaneous firing rate, by slightly depolarizing the membranes, whereas cathodal stimulation decreases cortical excitability by hyperpolarizing neurons' membranes. This mechanism of action was first illustrated by pioneering *in vivo* animal studies (Bindman, Lippold, & Redfearn, 1962; Creutzfeldt, Fromm, & Kapp, 1962; Purpura & McMurtry, 1965), showing that cortical excitability shifts depend on current polarity, stimulation intensity, as well as on the type and spatial orientation of the targeted neurons.

Long-lasting and polarity-dependent effects of tDCS were first explored in humans by stimulating the motor cortex and measuring the level of cortical excitability by means of motor evoked potentials (MEPs) by TMS (Nitsche & Paulus, 2001; Nitsche et al., 2005; Priori, Berardelli, Rona, Accornero, & Manfredi, 1998). The coupling of anodal-excitatory and cathodal-inhibitory effects are well established in the sensory and motor domains, both at physiological and behavioral levels, while evidence is more controversial for higher-level mental activity (Jacobson et al., 2012). Indeed, studies involving cognitive tasks show that while the anodal stimulation typically facilitates behavioral performance, the inhibitory effects of the cathodal stimulation are less consistent (Jacobson et al., 2012; Vallar & Bolognini, 2011).

On-line effects brought about by tDCS may be traced back to cellular mechanisms including membrane polarization. Conversely, longer-term after-effects may depend on LTP and LTD mechanisms, likely mediated by N-methyl-D-aspartate (NMDA) receptors and altering GABAergic activity and intracellular CA^{2+} concentration (Liebetanz et al., 2002; Nitsche, Fricke et al., 2003; Stagg et al., 2009). Indeed, the anodal after-effects are prolonged by the NMDA agonist D-Cycloserine (Nitsche, Jaussi et al., 2004), reduced by NMDA antagonist such as beta-adrenergic protanol (Nitsche et al., 2004), and abolished, irrespective of polarity, by NMDA-receptor-antagonist dextromethorphane. In addition to NMDA mechanisms, in a slice preparation of mouse motor cortex, anodal stimulation induced synaptic potentiation, depending on both brain-derived neurotrophic factor (BDNF) secretion, and tropomyosin-related kinase B (TrkB) activation (Fritsch et al., 2010). The long-term effects of tDCS also involve non-synaptic mechanisms arising from changes in pH and transmembrane proteins, which may alter neurons' membrane function (Ardolino, Bossi, Barbieri, & Priori, 2005).

Beyond shifting cortical excitability of the target area under the electrodes, tDCS may also affect cortical connectivity by modulating activity of distant brain regions, functionally or structurally connected to the stimulated area. For instance, Kirimoto et al., (2011) explored whether tDCS over the supplementary motor cortex modifies the excitability of ipsilateral primary motor (M1) and somatosensory (S1) cortices via neuronal connectivity, by measuring somatosensory evoked potentials (SEPs) and MEPs. Results showed that anodal tDCS decreased MEPs and increased SEPs amplitude, while cathodal stimulation yielded opposite effects.

Several studies recorded resting state electroencephalographic (EEG) and functional magnetic resonance imaging

(fMRI) activity in neurologically unimpaired participants, during or immediately after tDCS, in order to gather evidence concerning tDCS-induced regional cerebral activations or de-activations. For instance, a modulation of Visual Evoked Potentials (VEPs) amplitude was found both during and after tDCS, with effects dependent on the stimulation polarity and duration (Accornero, Voti, La Riccia, & Gregori, 2007; Antal, Kincses, Nitsche, Bartfai, & Paulus, 2004). In the language domain, Wirth and coauthors (2011) traced the neurophysiological underpinnings of the behavioral effects induced by anodal tDCS over left prefrontal cortex during a overt picture naming. Both behavioral and neurophysiological variables were tested during and after the end of the stimulation. An on-line enhancement of a language ERP component and an offline reduction of delta activity were reported, indicating that anodal tDCS induced an excitatory effect on frontally mediated neural processes and related language functions.

Lang et al., (2005) by means of PET, assessed the magnitude, duration and regional distribution of changes in regional Cerebral Blood Flow (rCBF), after tDCS stimulation over M1. When compared to sham tDCS, anodal and cathodal tDCS induced respectively widespread increases and decreases of rCBF in cortical and subcortical areas. Accordingly anodal tDCS over M1 increased rCBF, not only under the electrode, but also in a more widespread network, involving contralateral motor-related cortical areas (Zheng, Alsop, & Schlaug, 2011, using the arterial spin labeling technique).

Widespread activations induced by tDCS are in line with the observations made by computational models of current flow indicating that strong electric fields occur not only underneath and near the stimulating electrodes but also in the regions between them (Miranda, Mekonnen, Salvador, & Ruffini, 2013).

So far, our understanding of the precise electrophysiological effects of tDCS and how they spread across cortical networks is still far from being exhaustive (Brunoni et al., 2011). The combined use of neuroimaging techniques and tDCS can be crucial to improve our knowledge. In this perspective, we used an integrated TMS–Electroencephalography (TMS-EEG) system to explore the effects of anodal tDCS of the posterior parietal cortex (PPC). Global and local cortical excitability was assessed both on-line (i.e., during tDCS), and off-line (i.e., after 15 min from the end of the stimulation). The main advantage of this approach is to provide real-time and direct information on cortical reactivity, through TMS-evoked potentials (TEPs) recording and analysis. The PPC was chosen as TMS hotspot for two main reasons. First, we wanted to take advantage of the TMS-EEG technique, which allows exploring cortical reactivity of areas, such as the PPC, otherwise not functionally measurable, since they cannot produce a direct TMS output such as MEPs for M1 and phosphenes for the primary visual cortex (V1). Second, from a theoretical perspective, the PPC plays a key role in different sensorimotor and cognitive functions (Andersen & Cui, 2009; Critchley, 1953; Fogassi & Luppino, 2005; Ikkai & Curtis, 2011; Shomstein et al., 2012) and tDCS has been successfully applied to this area for modulating sensory (e.g., Bolognini, Fregni, Casati, Olgiati, & Vallar, 2010; Bolognini, Olgiati, Rossetti, & Maravita, 2010; Bolognini, Olgiati, Maravita, Ferraro, & Fregni, 2013; Convento, Vallar, Galantini, & Bolognini, 2013; Mancini,

Bolognini, Haggard, & Vallar, 2012) and cognitive (Berryhill, Wencil, Branch Coslett, & Olson, 2010; Sparing et al., 2009; Stone & Tesche, 2009) processing in healthy participants.

2. Material and Methods

2.1. Participants

Fourteen healthy, right-handed volunteers (four males, mean age 27 years, SD 5.9, range 22−38) participated in the study. Participants did not have any contraindication to noninvasive brain stimulation (Poreisz, Boros, Antal, & Paulus, 2007; Rossi, Hallett, Rossini, Pascual-Leone, & The Safety of TMS Consensus Group, 2009), namely no history of medical disorders, no substance abuse or dependence, no use of central nervous system-effective medication, and, particularly, no psychiatric and neurological disorders, including brain surgery, tumor, or intracranial metal implantation. All participants gave written informed consent prior to their participation in the study, which took place in the TMS-EEG laboratory of the University of Milano-Bicocca and was approved by the local Ethic Committee.

2.2. Procedure

For each participant, the experimental session consisted in three blocks of TMS-EEG recordings performed before (pre-tDCS), during (during-tDCS) and 15 min after anodal tDCS (post-tDCS) over the right PPC. Each recording lasted about 7 min during which each participant rested, fixating a white cross in black screen (17″) in front of him or her. TEPs were recorded starting from 2 msec after TMS pulse. Six participants underwent an additional session in which sham tDCS was delivered. The order of the two sessions (anodal and sham tDCS) was counterbalanced across subjects.

2.3. TMS stimulation

TMS was delivered with an Eximia™ TMS stimulator (Nexstim™, Helsinki, Finland) using a focal bi-pulse, figure of eight 70-mm coil. The site of stimulation was on the left PPC between P1 and CP1 electrodes. High-resolution (1 × 1 × 1 mm) structural magnetic resonance images (MRI) were acquired for each participant using a 3 T Intera Philips body scanner (Philips Medical Systems, Best, NL). TMS target was identified on individual MRI using a Navigated Brain Stimulation (NBS) system (Nexstim™, Helsinki, Finland), which employs infrared-based frameless stereotaxy, in order to map the position of the coil, and of the participant's head, within the reference space of the individual's MRI space. Mean MNI coordinates for the target site were $X = -31$ (SD $= 5.2$) $Y = -70$ (SD $= 6.6$) $Z = 54$ (SD $= 3.7$). The NBS system allowed to monitor continuously the position and orientation of the coil, thus assuring precision and reproducibility of the stimulation across sessions. Moreover, the NBS system estimated on-line the distribution and intensity (V/m) of the intracranial electric field induced by TMS, using a locally best-fitting spherical model, accounting for the head and brain shape of each participant, and taking into consideration the distance from scalp, coil position and orientation. Mean stimulation intensity, expressed as a

percentage of the maximal output of the stimulator, was 65%, (range = 60—78%), and corresponding to an an electric field of 106 ± 9 V/m. The coil was placed tangentially to the scalp, and adjusted for each participant in order to direct the electric field perpendicularly to the shape of the cortical gyrus/i, following the same procedure of previous studies (Casarotto et al., 2010; Mattavelli, Rosanova, Casali, Papagno, & Romero Lauro, 2013). Since TMS over parietal sites can activate temporal and frontal muscles, eliciting artifacts in the EEG recordings, the site of the stimulation was individually adjusted, in order to avoid or reduce as much as possible muscle twitches. TMS pulses were delivered at an inter-stimulus interval randomly jittered between 2000 and 2300 (.4—.5 Hz). Around 180 TMS pulses were delivered for each session.

2.4. tDCS

tDCS was delivered by a battery driven constant current stimulator (Eldith™,Neuroconn, Ilmenau, Germany) using a pair of rubber electrodes, covered with conductive paste (Ten20 conductive EEG paste, Kappamedical™, USA). An intracephalic montage was used. The anode (size = 9 cm^2; current density = .08 mA/cm^2) was placed over the right PPC underneath the EEG cap, through an eyelet in a site corresponding to P2 electrode, which was then removed (Fig. 1, panel A). The cathode (size = 25 cm^2, current density = .03 mA/cm^2) was positioned over the left supraorbital area. A constant current of .75 mA was applied for 15 min, with 8 s of fade-in/fade out period. Different sized electrodes were used to increase stimulation focality (Nitsche et al., 2008). For sham tDCS, the same electrode arrangement and parameters of stimulation were employed, but the stimulator was turned off after 30 s (Gandiga, Hummel, & Cohen, 2006).

The feasibility of concomitant EEG recording and tDCS application has been recently probed (Faria, Fregni, Sebastião, Dias, & Leal, 2012; Schestatsky, et al. 2013; Wirth, et al 2011). In order to avoid tDCS induced artifacts in the EEG trace, the tDCS electrodes and the conductive gel were never in contact
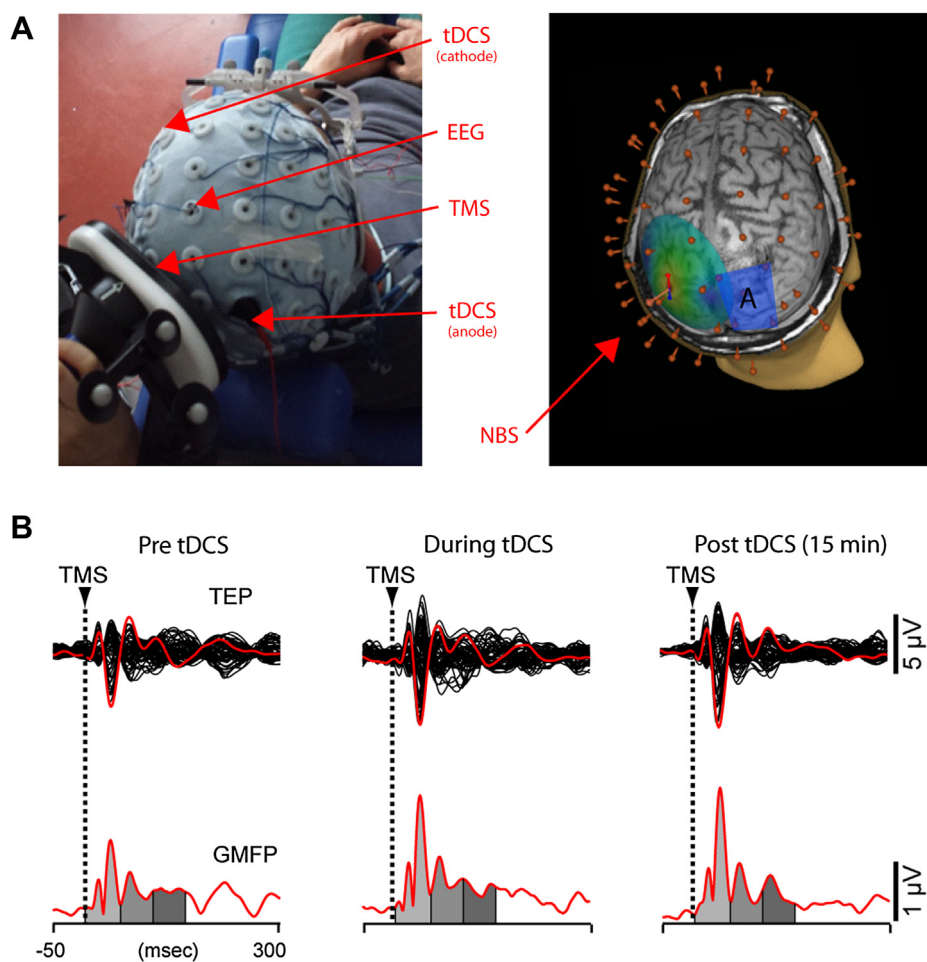

Fig. 1 — Panel A left represents a photo of the experimental setting adopted to deliver tDCS and TMS concurrently while recording EEG (during-tDCS condition). In the right bound a 3D reconstruction on the individual MRI is depicted showing the electrical field induced by TMS of the left parietal cortex, a blue rectangle representing the anode patch position over the right parietal cortex and 60 points corresponding to the EEG cap electrodes. Panel B reports the data from a representative subject and illustrates the procedure followed to compute the GMFP. In the upper bound the butterfly plot of the 60 channels' TEPs (upper bound) and the GMFP (red line in the lower bound) for the three conditions (pre-tDCS, during-tDCS, post-tDCS) are depicted. The TEP of the channel under the TMS is highlighted in red. The area beneath the curve of the GMFP was divided in three time windows: 0—50 msec (light gray), 50—100 msec (gray), 100—150 msec (dark gray).

with the surrounding EEG recording leads and faraway from both ground and refrence electrodes (placed on the forehead, see Fig. 1, panel A). Tansient EEG artifacts were observed only during the fade-in and fade-out phases of tDCS stimulation. TMS-EEG trials affected by those transient artifacts were rejected and, hence, did not contribute to the average TEPs.

2.5. EEG Recording during TMS

TEPs were continuously recorded using a TMS compatible 60-channels amplifier (Nexstim Ltd., Helsinki, Finland), which gates the TMS artifact and prevents saturation by means of a proprietary sample-and-hold circuit (Virtanen, Ruohonen, Naatanen, & Ilmoniemi, 1999). EEG signals were referenced to two electrodes placed over the forehead and used as ground. Eye movements were recorded with two additional electrodes placed near the eyes in order to monitor ocular artifacts. As in previous studies (Massimini et al., 2005; Casarotto et al., 2010), in order to prevent auditory potentials due to TMS pulse, a masking noise, which reproduce the TMS "click" in time-varying frequency components, was continuously played into earplugs worn by participants during the experimental sessions. Electrodes impedance was kept below 5 kΩ, and EEG signals were recorded with a sampling rate of 1450 Hz.

2.6. EEG data analysis

Data were pre-processed using Matlab R2011b® (Mathworks, Natick, MA, USA). First, recordings were down-sampled to 725 Hz. Continuous signal was then split in single trials starting 800 msec before the TMS pulse, and ending 800 msec after the TMS pulse. Trials with artifacts due to eye blinks/movements, spontaneous muscle activity or tDCS fade-in and fade-out phases were removed following a semi-automatic procedure (Casali, Casarotto, Rosanova, Mariotti, & Massimini, 2010), and the visual inspection of the signal by trained experimenters (G.M., S.C.). The average number of trials considered in the analysis was 155 (SD ± 14) for the pre-tDCS, 153 (SD ± 22) and 159 (SD ± 17) for the during- and post-tDCS conditions, respectively.

TEPs were computed by averaging selected artifact-free single trials and by filtering them between 2 and 40 Hz. Bad or missing channels were interpolated using spherical interpolation function of EEGLAB (Delorme & Makeig, 2004). TEPs were then referenced and baseline corrected between −300 and −50 msec before the TMS pulse.

For each condition, as an index of global excitability, Global Mean Field Power (GMFP) was computed on averaged TEPs of 60 channels for three temporal windows: 0—50 msec, 50—100 msec, 100—150 msec, with 0 msec corresponding to TMS pulse onset. The formula used to compute the GMFP was:

$$\text{GMFP}(t) = \sqrt{\left[\frac{\sum_i^k \left(V_i(t) - V_{mean(t)} \right) 2}{K} \right]}$$

where t is time, K the number of channels, V_i the voltage in channels averaged across subjects and V_{mean} is the mean of the voltages in all channels (Lehmann & Skrandies, 1980).

To further identify the specific contributions of different cortical regions to the increased global cortical excitability,

indexes of local excitability (Local Mean Field Power, LMFP) were measured and compared, following the same procedure used for GMFP. Six clusters of electrodes, each including 4 electrodes, were selected as follows based on anatomical locations: left frontal cluster (F1, F5, FC1, and FC3), right frontal cluster (F2, F6, FC2, and FC6), left parietal cluster, corresponding to TMS hotspot (CP1, CP3, P1, and P3), right parietal cluster near tDCS anode (CP2, CP4, P2, and P4), left temporal (FT7 FC5 T3 C5) and right temporal (FC6 FT8 C6 T4) clusters. In order to obtain a synthetic index of global and local cortical excitability, GMFP and LMFP values were cumulated within three time windows (0—50 msec, 50—100 msec, 100—150 msec after the TMS pulse) and for each experimental condition (pre-, during- and post-tDCS). Integrated GMFP and LMFP within the three time-windows after the TMS pulse were then log-transformed (log-GMFP and log-LFMP) to obtain normally distributed data (Shapiro—Wilk test $p > .05$).

Pre-, during- and post-tDCS GMFP values were then compared in each time window by means of repeated measures Analysis of Variance (ANOVA), with log-GMFP, as dependent variable, and Condition (pre-tDCS, during-tDCS, post-tDCS) as within factor.

Accordingly, log-LMFP for each time window was introduced as dependent variable in separate repeated measures ANOVAs with Cluster (6 levels: left/right frontal, parietal and temporal) and Condition (3 levels: pre-tDCS, during-tDCS, post-tDCS) as within subjects factors. Bonferroni correction was applied for post-hoc planned comparisons.

To further analyze whether the global effect was driven by certain locations affecting the average signal across all channels, GMFP was also computed on averaged TEPs of 60 channels minus the four clusters (right/left for frontal/parietal) in which significant changes across conditions were found. These data were analyzed via a repeated-measures ANOVA in order to compare pre-, during- and post-tDCS GMFP values in the three identified time windows. For sake of clarity, the results of this analysis are listed in the GMFP paragraph (3.1.2).

3. Results

Fig. 1A shows the experimental set-up and the NBS positioning system, and Fig. 1B the EEG responses, recorded at the 60 electrodes (black traces), when TMS was applied over the PPC in one representative participant. The TEPs recorded at the electrode under the stimulator is shown in red trace. As already found in previous studies (Rosanova et al. 2009, Ferrarelli et al. 2012), TEPs waveform following PPC stimulation are characterized by two negative components within the first 100 msec. This pattern is reproducible across participants and conditions (pre-tDCS, during-tDCS and post-tDCS).

3.1. Global excitability shifts by anodal tDCS

3.1.1. 60 channels
In the early 0—50 msec time window, the main effect of Condition was significant [$F(2,26) = 12.28$, $p = .000$, $p\eta^2 = .49$] with an increase during-tDCS ($p = .015$) and post-tDCS ($p = .001$), as compared to pre-tDCS.

In the 50–100 msec time window, the main effect of Condition was significant [$F(2,26) = 6.39$, $p = .005$, $p\eta^2 = .33$]. Post-hoc comparison showed significantly higher values during-tDCS ($p = .002$) and post-tDCS ($p = .041$), as compared to pre-tDCS.

In the late 100–150 msec time window, instead, the main effect of Condition was not significant [$F(2,26) = .42$, $p = .66$, $p\eta^2 = .03$] (Fig. 2).

3.1.2.   60 Channels minus parietal/frontal right/left clusters

This analysis confirmed the results found in 60 channels. The main effect of condition was significant in both the 0–50 msec [$F(2,26) = 8.66$, $p = .001$, $p\eta^2 = .40$] and 50–100 msec [$F(2,26) = 6.75$, $p = .003$, $p\eta^2 = .34$] time windows.

Post-hoc comparisons showed a significant increase of the global cortical excitability index in the two time windows between 0 and 100 msec, both during-tDCS and post-tDCS condition as compared to pre-tDCS. No significant change across conditions was found in the late temporal window 100–150 msec (see Table A.1 in appendix for a detailed list of p values found).

3.2.   Local excitability shifts by anodal tDCS

3.2.1.   Time window 0–50 msec

The ANOVA run on log-LMFP in the first time window (0–50 msec) showed a significant main effect of Cluster [$F(5, 65) = 14.78$, $p = .000$, $p\eta^2 = .53$], with greater values for the left parietal and left frontal clusters, significantly higher than the right parietal cluster. The increased LMFP in these clusters is likely due to the TMS hotspot location.

The main effect of Condition was significant [$F(2, 26) = 12.36$, $p = .000$, $p\eta^2 = .48$], with post-tDCS values significantly greater than the pre-tDCS ones ($p = .000$). The interaction Cluster X condition was not significant [$F(10, 130) = .46$, $p = .91$, $p\eta^2 = .03$] suggesting that the same trend across conditions was present in each cluster. However, since our aim was to examine the pattern of tDCS effects across different

locations, we also compared the three conditions for each cluster, by means of post-hoc planned comparisons (Fig. 3). Post-tDCS values significantly increased, as compared to pre-TDCS, in the bilateral frontal ($p = .01$) and parietal clusters (left: $p = .002$; right: $p = .02$), but not in the temporal ones (see Table A.2 in appendix for a list of all p values found).

3.2.2.   Time window 50–100 msec

The main effect of Cluster was not significant [$F(5, 65) = 1.51$, $p = .19$, $p\eta^2 = .10$]. The main effect of Condition was significant [$F(2, 26) = 7.34$, $p = .003$, $p\eta^2 = .36$] with during-tDCS ($p = .002$) and post-tDCS ($p = .009$) conditions showing greater values than pre-tDCS recordings. The interaction between Cluster and Condition was not significant [$F(10, 130) = .78$, $p = .64$].

As for 0–50 msec time window, planned post-hoc comparisons among conditions were run for each cluster. Significant changes were found only in the right temporal cluster, where the during-tDCS condition was greater than the pre-tDCS ($p = .015$).

3.2.3.   Time window 100–150 msec

The main effect of Cluster was significant [$F(5, 65) = 6.24$, $p = .000$, $p\eta^2 = .32$], with significantly higher LMFP for the right temporal cluster than the right parietal ($p = .012$) and left temporal ($p = .005$) clusters. Neither the Condition [$F(2,26) = .83$, $p = .44$, $p\eta^2 = .00$], nor the interaction Cluster X condition were significant [$F(2, 26) = 1.11$, $p = .36$, $p\eta^2 = .08$].

Planned post-hoc comparisons among the three conditions within each cluster did not show any significant change between conditions (see Table A.2 for p values).

3.3.   Sham TDCS

3.3.1.   Global excitability

Regarding GMFP, the main effect of Condition was not significant in any temporal window: 0–50 msec: $F(2,10) = .16$,
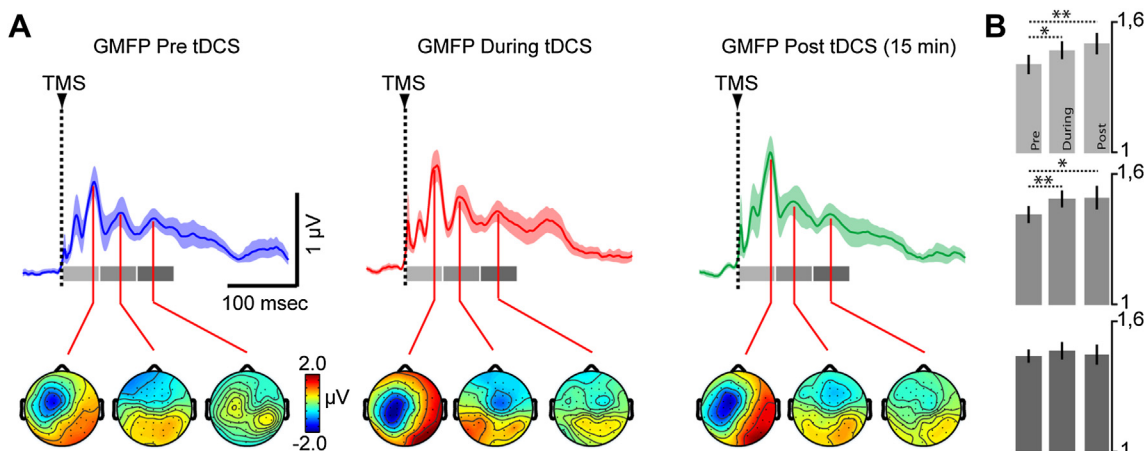
Fig. 2 – Panel A (upper row) shows the Grand Average of GMFP computed by averaging the GMFPs calculated for each subject in the three experimental conditions (pre tDCS = blue trace ± SE; during tDCS = red trace ± SE; post tDCS = green trace ± SE). The lower row of Panel A represents the mean topographies computed in correspondence of the local maxima for each of the three time windows (0–50 msec = light gray, 50–100 msec = gray, 100–150 msec = dark gray) across the 14 study participants (see also Fig. 1). Panel B shows bar histograms representing the mean values ± SE of the integrated GMFP in the three time windows of interest (0–50 msec = light gray, 50–100 msec = ash, 100–150 msec = graphite) for each experimental condition.
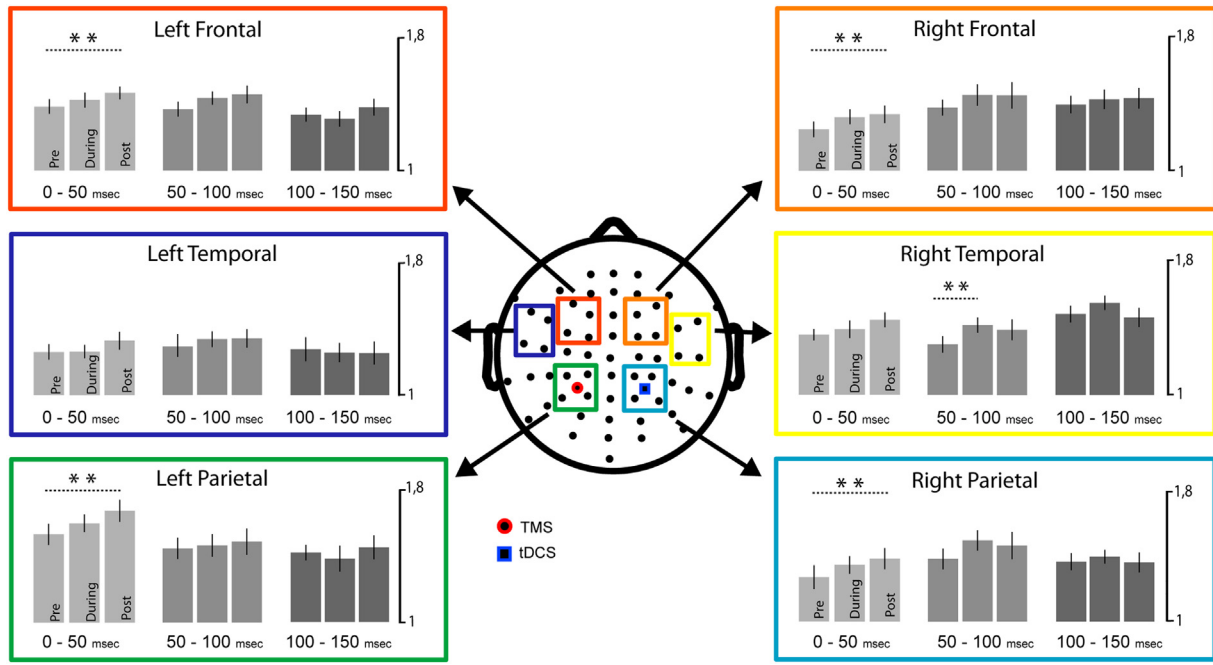
Fig. 3 — Mean log-LMFP for the six clusters of interest are shown. Colored squares on the head model represent the clusters of electrodes analyzed in the parietal, frontal and temporal regions. The red dot in the left parietal cluster represents TMS target location while the blue square in the right parietal region represents tDCS anode location. For each colored square the bar graphs represent mean log-LMFP in the baseline, during and post tDCS conditions for the three temporal windows identified: 0–50 msec (light gray), 50–100 msec (gray) and 100–150 msec (dark gray). Error bars represent the standard error. * and ** represent significant differences between condition at $p < .05$ and $p < .02$ respectively.

$p = .85$, $p\eta^2 = .03$; 50–100 msec: $F(2,10) = .22$, $p = .81$, $p\eta^2 = .04$; 100–150 msec: $F(2,10) = .37$, $p = .96$, $p\eta^2 = .00$].

3.3.2. Local excitability

For all the considered time windows, the main effect of Cluster was significant: 0–50 msec, $F(5,25) = 4.92$, $p = .003$, $p\eta^2 = .49$; 50–100 msec, $F(5,25) = 2.98$, $p, = .03$, $p\eta^2 = .37$; 100–150 msec, $F(5,25) = 7.91$, $p = .000$, $p\eta^2 = .61$]. *Post-hoc* showed a non-significant trend toward higher LMFP in the left parietal cluster in the 0–100 msec interval (all *ps* > .12), and in the right temporal cluster in the later window (all *ps* > .09). The main effect of Condition, and the Cluster × Condition interaction, were not significant in any temporal window (all *ps* > .57).

4. Discussion

To the best of our knowledge, this is the first study in which TMS and compatible continuous EEG recording is used to investigate on-line and after-effects of tDCS on a region outside the motor system. Our results show that, at a global level (i.e., GMFP), anodal tDCS of the right PPC increases cortical excitability in a temporal window of 0–100 msec both during and 15 min after the end of the stimulation. At the local level, anodal tDCS of the right PPC induces off-line widespread enhancements of neural excitability in the earlier components of TEPs (0–50 msec) in the

targeted right PPC, as well as in the contralateral homolog area and bilaterally in the frontal regions; instead, no modulatory effects were found in right and temporal areas. Later components (100–150 msec) are increased on-line in the right temporal area.

In particular, the first remarkable finding is probing the feasibility of using TMS-EEG to track changes in cortical excitability and connectivity induced by tDCS, both during and after the end of the stimulation. The combination of tDCS and TMS-EEG as a "multimodal imaging approach" appears indeed promising (Miniussi, Brignani, & Pellicciari, 2012). TMS allows exploring how the reactivity of a target area is modulated by tDCS. Combining TMS end EEG permits to trace these changes in any cortical area, by means of TEPs, which are considered as reliable measures of brain activation state (Miniussi & Thut, 2010). Moreover the high-definition of EEG recording permits to prove the state of broader cortical networks, unveiling how activation spreads to interconnected areas. As long as the same parameters across sessions are maintained, the reliability of the technique has been probed (Casarotto et al., 2010), allowing to link any observed changes in TEPs to the tDCS effects, rather than to any other confounding factor. Moreover, in this study the lack of changes when sham tDCS, instead of real tDCS, is delivered, allows to exclude the intervention of unspecific effects, such as boredom or fatigue, further confirming the reliability of the TMS-EEG approach.

The GMFP increment from pre-tDCS within the 0−100 msec interval during-tDCS and after-tDCS survives to the removing from the analysis of the four clusters, namely the right and left parietal and frontal clusters, where the main significant local effects took place. Therefore, the increment of GMFP cannot merely be the result of local signal changes.

Here, both global and local excitability analyses show that anodal tDCS significantly modulates the earlier stages of GMFP/LMFP, in the 0−50 msec time window. TEPs components that are evoked within the first 50 msec after the TMS pulse directly reflect the excitability of the stimulated cortical area and of those areas monosynaptically connected to the target area (Ilmoniemi et al., 1997). Notably, the amplitude of these early components of TEPs significantly increases after the application of the rTMS at 5 Hz (Esser et al., 2006), after electroconvulsive therapy (Casarotto et al., 2013), and they are modulated by wakefulness−sleep cycle (Huber et al., 2013). Previous studies found that anodal tDCS of the motor cortex elicits a sustained increase of cortical excitability, as measured by TMS-induced MEPs (Nitsche & Paulus, 2000, 2001; Nitsche, Liebetanz et al., 2003). Similarly, tDCS is effective in modulating early components of evoked cortical activity. For instance, Antal et al. (2004), evaluated the polarity-specific effects of tDCS of V1, by measuring VEPs before and after (i.e., 10, 20, 30 min) tDCS, assessing the influence of different parameters, such as current polarity, duration of stimulation, electrode montage. Anodal tDCS increased early occipital responses (i.e., N70), while cathodal tDCS decreased it. As in the present study, the effects of the anodal stimulation emerges only 10 min after the end of a stimulation, and lasts for 15 min. Similarly, anodal tDCS on the somatosensory and temporo-parietal cortices elicits a prolonged increment of parietal and frontal SEPs, and increases temporal auditory evoked potentials within the first 50 msec (Kirimoto et al., 2011; Matsunaga, Nitsche, Tsuji, & Rothwell, 2004; Zaehle, Beretta, Jancke, Herrmann, & Sandmann, 2011).

Here, both global and local indexes of cortical excitability indicate that the effects of tDCS are diffuse, rather than being restricted to the area underneath the active electrode. These findings are in line with previous studies measuring the effect of anodal tDCS over the motor cortex, as assessed by means of EEG recording (Kirimoto et al., 2010), and fMRI/PET during task performance (Lang et al., 2005; Stagg et al., 2009; Polania, Nitsche, & Paulus, 2011) or during a resting state (Lang et al., 2005; Polania, Paulus, Antal, & Nitsche, 2011; Zheng et al., 2011). Therefore, tDCS can modulate cortical activity both within the region directly under the stimulating electrode, as well as in regions anatomically connected, but spatially distant. Similarly, tDCS delivered over the dorsolateral prefrontal cortex (DLPFC) induces widespread changes involving distinct network beyond the stimulation site (Keeser et al., 2011, Keeser, Padberg et al., 2011; Pena-Gomez et al., 2012). Stagg et al. (2013), for instance, investigated brain perfusion changes during tDCS applied to the left DLPFC in healthy humans, using whole-brain arterial spin labeling. An increased perfusion in regions anatomically connected to the DLPFC, in conjunction with a decreased functional coupling between the left DLPFC and the thalami bilaterally, was found. Interestingly, the effects during and after tDCS were markedly different: a widespread decrease in cortical perfusion was found after both anodal and cathodal tDCS, as compared to during tDCS (Stagg et al., 2013). Notably, caution is warranted in interpreting results from neuroimaging studies tracking the neurophysiological effects of tDCS, since there is a potential confounding artifact by the magnetic field deriving from tDCS current flow, as revealed by a study of tDCS effects in post-mortem brain, using a conventional echo-planar imaging sequence (Antal et al., 2012). Since in dead subjects hemodynamic changes in brain activity are obviously absent, any detected signal resulted from the applied currents. In this perspective, the present results provide instead a stronger evidence of the modulatory tDCS effects on cortical excitability, through a direct measure of it by means of TMS-EEG.

The widespread effect of tDCS are in line with a computational model of the electrical field for the montage used in the present study (see Fig. A.1 in the appendix). It is indeed known that the electrodes montage critically affects the distribution of the electrical current in the brain (Miranda et al., 2006; Faria, Leal, & Miranda, 2009). In line with GMFP/LMFP results, the MRI-based modeling of transcranial current flow indicates a widespread distribution of the electric field, in which the maximal stimulation in the brain volume does not occur only under the stimulation sites, but also between the two cephalic electrodes.

In the present study, local excitability analysis showed that the after-effects of anodal tDCS resulted in a shift of cortical excitability within ipsilateral and bilateral fronto-parietal networks. Since participants were at rest during the TMS-EEG recording, the diffusion of tDCS after-effects are likely to reflect structural, rather than functional task-dependent, connections among parietal and frontal areas. The effect on the contralateral homolog parietal cortex (i.e., left parietal cluster) likely depends on callosal connections, which provide the majority of axonal transmissions between the two hemispheres (Doron & Gazzaniga, 2008). A recent study (Pellicciari, Brignani, & Miniussi, 2013) investigated cortical excitability immediately and 30 min after anodal and cathodal tDCS over left M1. Both TEPs and MEPs were measured. Results showed that tDCS modulated in a polarity-dependent fashion both cortical and corticospinal excitability, with changes in cortical reactivity emerging immediately after the end stimulation and after 30 min, although reduced. Moreover, anodal tDCS (as well as cathodal) increased cortical excitability also in the contralateral hemisphere. Our findings further support the view that unilateral anodal tDCS can affect inter-hemispheric interactions, hence suggesting that the behavioral benefits of this stimulation, in both healthy and brain-damaged individuals, are likely supported not only by a local modulation of the activity in the targeted area, but also by distant effects in homologs areas of the contralateral hemisphere, through a trans-callosal physiological modulation.

The off-line tDCS increment of excitability in ipsilateral and contralateral frontal cortices, without corresponding changes in temporal regions, suggests that although widespread, the tDCS after-effects are mainly restring to a fronto-parietal network, likely corresponding to a default mode brain network known to be a dynamic baseline (not stimulus-related or task-related) of intrinsic brain activity during resting wakefulness (Chen, Feng, Zhao, Yin, & Wang, 2008; Gusnard & Raichle, 2001).

Notably, the on-line GMFP (i.e., during tDCS) increment in the 0–100 msec interval is not found in the LMFP analysis, with the exception of the right temporal cluster showing significantly greater LMFP (50–100 msec interval) during tDCS, as compared to baseline. We hypothesize that on-line tDCS effect might be more diffuse and feeble to be detected at a cluster level, thus only including a small number of electrodes. The broader diffusion of the effects during stimulation might be due to the current passage, which induced, as shown by our model, a widespread electrical field. Off-line effects might instead be preferentially directed along a fronto-parietal network, thus becoming significant in our LMFP analysis.

The neurophysiological evidence of a widespread effect may seem in contrast with a growing body of evidence showing the selectivity of tDCS effects on behavior. However, such behavioral specificity of tDCS (Vallar & Bolognini, 2011; Nitsche & Paulus, 2011) may depend on the baseline (active vs non-active) state of the stimulated cortical area. In a recent study (Polania et al., 2011), functional connectivity and graph theoretical analysis in EEG recordings were used to track changes in the motor cortical network induced by anodal tDCS of the motor cortex, comparing changes in a resting state versus task-related (i.e., finger tapping task) changes. Although anodal tDCS altered both intra-hemispheric and inter-hemispheric connectivity within a large sensori-motor network in multiple frequency bands, a specific increase of functional connectivity at the high-gamma frequency band (60–90 Hz) was found after tDCS only during the execution of the motor task, but not in the resting state. Therefore, the suggestion has been made that the strengthening of synaptic connections, i.e., functional connectivity, requires the interaction between the tDCS effects and the task-dependent effects. In line with this suggestion, anodal tDCS applied to M1 does not improve motor skill learning in the absence of training, indicating that ongoing synaptic activity induced by practice is a prerequisite for the emergence of tDCS-induced behavioral benefits (Fritsch et al., 2010). Overall, the effects of tDCS may differ depending on their association with the on-going behavioral activity (e.g., sensory, motor, or higher-order behavioral task). This is an issue that warrants further instigation in order to maximize the behavioral improvement induced by tDCS (e.g., Bolognini et al., 2009).

In conclusion, our study support the view that on-line neurophysiological tDCS effects are relatively diffuse, whereas off-line tDCS effects preferentially affect networks, defined by ipsilateral and contralateral structural or functional connections, according to the resting versus active state of the subject during the stimulation. Notably, the TMS-EEG provides a direct measure of cortical excitability,

however, caution is warranted in interpreting the results of local signal effects, due to the poor spatial resolution of the EEG. Source modeling analysis (Casarotto et al., 2010) can account for this limitation, thus a future direction for this study would be to further explore the precise spatial localization of the local tDCS effects.

Acknowledgments

Appendix

TDCS computational model

A realistic MR derived finite element model as described in Opitz, Windhoff, Heidemann, Turner, and Thielscher (2011) was used to simulate the electric field distribution using SimNibs (Windhoff, Opitz, & Thielscher, 2013). Five different tissue types including WM, GM, CSF, skull and skin were distinguished. Isotropic conductivities were used as follows: $\sigma_{skin} = .25$ S/m, $\sigma_{skull} = .008$ S/m, $\sigma_{CSF} = 1.79$ S/m, $\sigma_{GM} = .276$ S/m and $\sigma_{WM} = .126$ S/m. The electrode montage was modeled such as applied during the experiment (see Fig. A.1, Panel A). The electric field distribution in the brain is shown in Fig. A.1, Panel B. While the strongest electric field strengths occur around the area underneath the electrodes, enhanced electric fields also occur in a large cortical area between the electrodes.
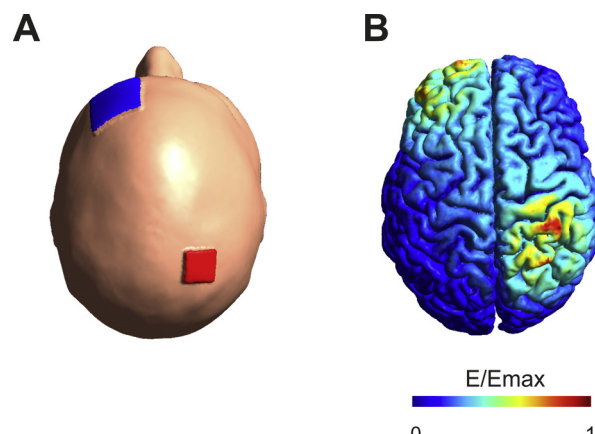
Fig. A.1 – Computational model of the electric field during tDCS: A) Modeled montage including the anode (red) over the right PPC and the anode (blue) over the contralateral sopraorbital area. B) Simulated absolute electric field in the brain. The strongest electric field occurs around the cortical area underneath the anode. Large electric field strengths take place also at the site of the cathode and between the electrodes.

Sham

0-50 ms

Anodal
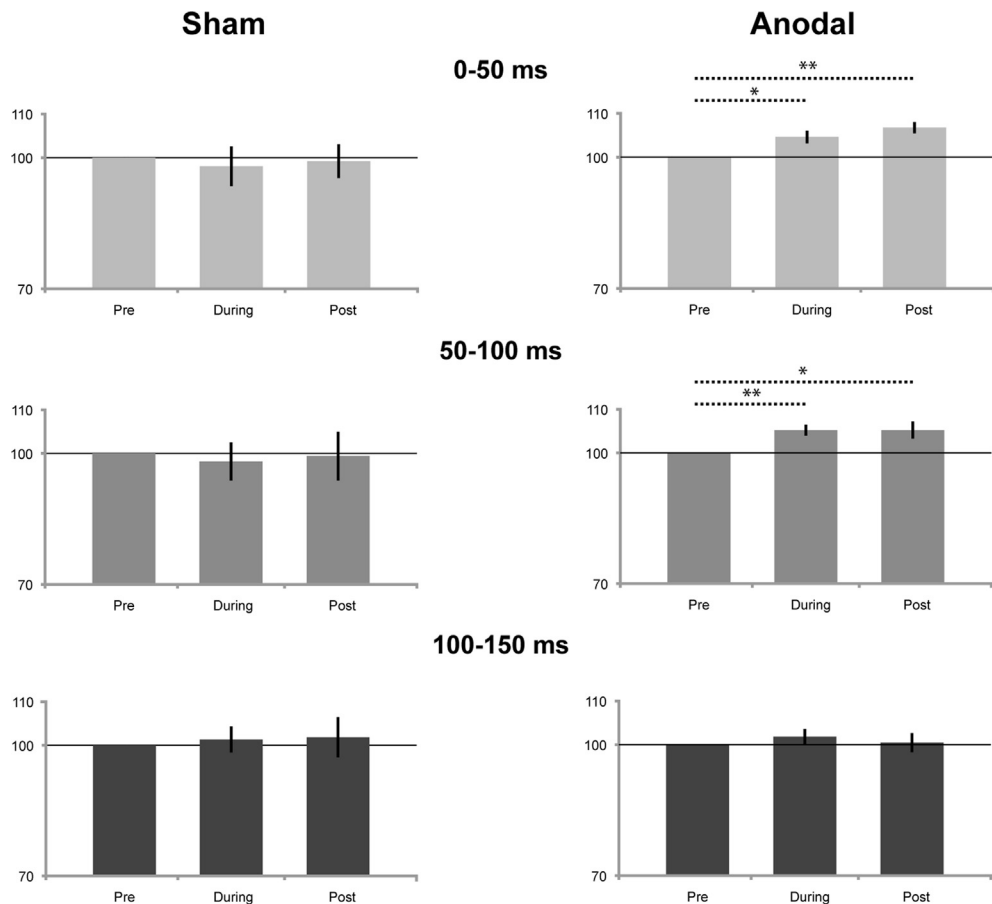
50-100 ms

100-150 ms

Fig. A.2 — Bar histograms representing the mean values ± SE of the integrated GMFP plotted as percentage of the pre-TDCS condition in the three time windows of interest (0–50 msec = light grey, 50–100 msec = ash, 100–150 msec = graphite) after sham and anodal TDCS stimulation. Whereas after anodal TDCS in the 0–100 ms interval the during − and post-TDCS conditions significantly increased in comparison to pre-TDCS, no difference was found among the conditions in any temporal interval when SHAM tDCS was delivered. * and ** indicate significant differences between conditions at *p* < .05 and *p* < .02 respectively.

Table A.1 — A list of *p* values is reported resulting from the post-hoc comparisons (Bonferroni corrected) between during-tDCS versus pre-tDCS (Dur *vs* pre) and post-tDCS versus pre-tDCS (Post *vs* pre) in several analyses (in the head of the columns, from left to right): GMFP after anodal tDCS computed on 60 channels; GMFP after sham stimulation, computed on 60 channels; GMFP after anodal tDCS computed on 60 channels minus 4 clusters, namely left/right (L/R) parietal/frontal; GMFP after anodal tDCS computed on 60 channels minus the left frontal cluster; minus the right frontal cluster; minus the left parietal cluster (TMS site); minus the right parietal cluster (tDCS anode site). The analyses were run separately for the three time windows: 0–50 msec, 50–100 msec and 100–150 msec.

GMFP		60 channels	Sham: 60 channels	Without 4 clusters	Without L frontal cluster	Without R frontal cluster	Without L pariet. Cluster	Without R pariet. Cluster
0–50	Dur versus pre	*p* = .015	*p* = 1.00	*p* = .03	*p* = .008	*p* = .015	*p* = .014	*p* = .01
	Post versus pre	*p* = .000	*p* = 1.00	*p* = .003	*p* = .002	*p* = .002	*p* = .008	*p* = .002
50–100	Dur versus pre	*p* = .002	*p* = 1.00	*p* = .001	*p* = .001	*p* = .000	*p* = .001	*p* = .002
	Post versus pre	*p* = .041	*p* = 1.00	*p* = .03	*p* = .093	*p* = .10	*p* = .09	*p* = .09
100–150	Dur versus pre	*p* = 1.00	*p* = 1.00	*p* = .93	*p* = .79	*p* = .88	*p* = .77	*p* = .85
	Post versus pre	*p* = 1.00	*p* = 1.00	*p* = 1.00	*p* = 1.00	*p* = 1.00	*p* = 1.00	*p* = 1.00

Table A.2 − A list of *p* values is reported resulting from the post-hoc planned comparisons (Bonferroni corrected) between during-tDCS versus pre-tDCS (Dur *vs* Pre) and post-tDCS versus pre-tDCS (Post *vs* Pre) performed for each time window separately within each cluster of interest (in the head of the columns, from left to right): Left frontal cluster (F1, F5, FC1 and FC3); right frontal cluster (F2, F6, FC2, and FC6); left parietal cluster (TMS site; CP1, CP3, P1, and P3); right parietal cluster (tDCS anode; CP2, CP4, P2, and P4); left temporal (FT7 FC5 T3 C5); right temporal (FC6 FT8 C6 T4).

LMFP		Left frontal	Right frontal	Left parietal	Right parietal	Left temporal	Right temporal
0−50	Dur versus pre	$p = .32$	$p = .47$	$p = .14$	$p = .59$	$p = 1.00$	$p = 1.00$
	Post versus pre	$p = .014$	$p = .015$	$p = .002$	$p = .022$	$p = .59$	$p = .10$
50−100	Dur versus pre	$p = .095$	$p = .56$	$p = 1.00$	$p = .15$	$p = 1.00$	$p = -015$
	Post versus pre	$p = .34$	$p = .40$	$p = .99$	$p = .23$	$p = .87$	$p = .18$
100−150	Dur versus pre	$p = 1.00$	$p = 1.00$	$p = 1.00$	$p = .14$	$p = 1.00$	$p = .21$
	Post versus pre	$p = 1.00$	$p = 1.00$	$p = 1.00$	$p = .57$	$p = 1.00$	$p = 1.00$

REFERENCES

Accornero, N., Voti, P. L., La Riccia, M., & Gregori, B. (2007). Visual evoked potentials modulation during direct current cortical polarization. *Experimental Brain Research, 178*(2), 261−266.

Andersen, R. A., & Cui, H. (2009). Intention, action planning, and decision making in parietal-frontal circuits. *Neuron, 63*(5), 568−583.

Antal, A., Bikson, M., Datta, A., Lafon, B., Dechent, P., Parra, L. C., et al. (2012). Imaging artifacts induced by electrical stimulation during conventional fMRI of the brain. *NeuroImage, 85*, 1040−1047.

Antal, A., Kincses, T. Z., Nitsche, M. A., Bartfai, O., & Paulus, W. (2004). Excitability changes induced in the human primary visual cortex by transcranial direct current stimulation: direct electrophysiological evidence. *Investigative Ophthalmology & Visual Science, 45*(2), 702−707.

Antal, A., Lang, N., Boros, K., Nitsche, M., Siebner, H. R., & Paulus, W. (2008). Homeostatic metaplasticity of the motor cortex is altered during headache-free intervals in migraine with aura. *Cerebral Cortex, 18*(11), 2701−2705.

Antal, A., Paulus, W., & Nitsche, M. A. (2011). Electrical stimulation and visual network plasticity. *Restorative Neurology and Neuroscience, 29*(6), 365−374.

Ardolino, G., Bossi, B., Barbieri, S., & Priori, A. (2005). Non-synaptic mechanisms underlie the after-effects of cathodal transcutaneous direct current stimulation of the human brain. *The Journal of Physiology, 568*(Pt 2), 653−663.

Berryhill, M. E., Wencil, E. B., Branch Coslett, H., & Olson, I. R. (2010). A selective working memory impairment after transcranial direct current stimulation to the right parietal lobe. *Neuroscience Letter, 479*(3), 312−316.

Bindman, L. J., Lippold, O. C., & Redfearn, J. W. (1962). Long-lasting changes in the level of the electrical activity of the cerebral cortex produced bypolarizing currents. *Nature, 196*, 584−585.

Boggio, P. S., Rigonatti, S. P., Ribeiro, R. B., Myczkowski, M. L., Nitsche, M. A., Pascual-Leone, A., et al. (2008). A randomized, double-blind clinical trial on the efficacy of cortical direct current stimulation for the treatment of major depression. *The International Journal of Neuropsychopharmacology, 11*(2), 249−254.

Bolognini, N., Fregni, F., Casati, C., Olgiati, E., & Vallar, G. (2010). Brain polarization of parietal cortex augments training-induced improvement of visual exploratory and attentional skills. *Brain Research, 1349*, 76−89.

Bolognini, N., Olgiati, E., Maravita, A., Ferraro, F., & Fregni, F. (2013). Motor and parietal cortex stimulation for phantom limb pain and sensations. *Pain, 154*(8), 1274−1280.

Bolognini, N., Olgiati, E., Rossetti, A., & Maravita, A. (2010). Enhancing multisensory spatial orienting by brain polarization of the parietal cortex. *European Journal of Neuroscience, 31*(10), 1800−1806.

Bolognini, N., Pascual-Leone, A., & Fregni, F. (2009). Using non-invasive brain stimulation to augment motor training-induced plasticity. *Journal of Neuroengineering and Rehabilitation, 6*, 8.

Brunoni, A. R., Ferrucci, R., Bortolomasi, M., Vergari, M., Tadini, L., Boggio, P. S., et al. (2011). Transcranial direct current stimulation (tDCS) in unipolar vs. bipolar depressive disorder. *Progress in Neuro-psychopharmacology & Biological Psychiatry, 35*(1), 96−101.

Casali, A. G., Casarotto, S., Rosanova, M., Mariotti, M., & Massimini, M. (2010). General indices to characterize the electrical response of the cerebral cortex to TMS. *NeuroImage, 49*(2), 1459−1468.

Casarotto, S., Canali, P., Rosanova, M., Pigorini, A., Fecchio, M., Mariotti, M., et al. (2013). Assessing the effects of electroconvulsive therapy on cortical excitability by means of transcranial magnetic stimulation and electroencephalography. *Brain Topography, 26*(2), 326−337.

Casarotto, S., Romero Lauro, L. J., Bellina, V., Casali, A. G., Rosanova, M., Pigorini, A., et al. (2010). EEG responses to TMS are sensitive to changes in the perturbation parameters and repeatable over time. *PLoS One, 5*(4), e10281.

Chen, A. C. N., Feng, W., Zhao, H., Yin, Y., & Wang, P. (2008). EEG default mode network in the human brain: spectral regional field powers. *NeuroImage, 41*, 561−574.

Convento, S., Vallar, G., Galantini, C., & Bolognini, N. (2013). Neuromodulation of early multisensory interactions in the visual cortex. *Journal of Cognitive Neuroscience, 25*(5), 685−696.

Creutzfeldt, O. D., Fromm, G. H., & Kapp, H. (1962). Influence of transcortical d-c currents on cortical neuronal activity. *Experimental Neurology, 5*, 436−452.

Critchley, M. (1953). *The parietal lobes*. London: Edward Arnold.

Dasilva, A. F., Mendonca, M. E., Zaghi, S., Lopes, M., Dossantos, M. F., Spierings, E. L., et al. (2012). tDCS-induced analgesia and electrical fields in pain-related neural networks in chronic migraine. *Headache, 52*(8), 1283−1295.

Delorme, A., & Makeig, S. (2004). EEGLAB: an open source toolbox for analysis of single-trial EEG dynamics including independent component analysis. *Journal of Neuroscience Methods, 134*, 9−21.

Doron, K. W., & Gazzaniga, M. S. (2008). Neuroimaging techniques offer new perspectives on callosal transfer and interhemispheric communication. *Cortex, 44*(8), 1023−1029.

Esser, S. K., Huber, R., Massimini, M., Peterson, M. J., Ferrarelli, F., & Tononi, G. (2006). A direct demonstration of cortical LTP in humans: a combined TMS/EEG study. *Brain Research Bulletin, 69*(1), 86−94.

Faria, P., Fregni, F., Sebastião, F., Dias, A. I., & Leal, A. (2012). Feasibility of focal transcranial DC polarization with simultaneous EEG recording: Preliminary assessment in healthy subjects and human epilepsy. *Epilepsy & Behavior, 25*(3), 417−425.

Faria, P., Leal, A., & Miranda, P. C. (2009). Comparing different electrode configurations using the 10-10 international system in tDCS: a finite element model analysis. In *Conf Proc IEEE Eng Med Biol Soc, 2009* (pp. 1596–1599).

Ferrarelli, F., Sarasso, S., Guller, Y., Riedner, B. A., Peterson, M. J., Bellesi, M., et al. (2012). Reduced natural oscillatory frequency of frontal thalamocortical circuits in schizophrenia. *Archives of General Psychiatry, 69*(8), 766–774.

Ferrucci, R., Bortolomasi, M., Vergari, M., Tadini, L., Salvoro, B., Giacopuzzi, M., et al. (2009). Transcranial direct current stimulation in severe, drug-resistant major depression. *Journal of Affective Disorders, 118*(1–3), 215–219.

Ferrucci, R., Mameli, F., Guidi, I., Mrakic-Sposta, S., Vergari, M., Marceglia, S., et al. (2008). Transcranial direct current stimulation improves recognition memory in Alzheimer disease. *Neurology, 71*(7), 493–498.

Fogassi, L., & Luppino, G. (2005). Motor functions of the parietal lobe. *Current Opinion in Neurobiology, 15*(6), 626–631.

Fregni, F., Boggio, P. S., Santos, M. C., Lima, M., Vieira, A. L., Rigonatti, S. P., et al. (2006). Noninvasive cortical stimulation with transcranial direct current stimulation in Parkinson's disease. *Movement Disorders, 21*(10), 1693–1702.

Fregni, F., Thome-Souza, S., Nitsche, M. A., Freedman, S. D., Valente, K. D., & Pascual-Leone, A. (2006). A controlled clinical trial of cathodal DC polarization in patients with refractory epilepsy. *Epilepsia, 47*(2), 335–342.

Fritsch, B., Reis, J., Martinowich, K., Schambra, H. M., Ji, Y., Cohen, L. G., et al. (2010). Direct current stimulation promotes BDNF-dependent synaptic plasticity: potential implications for motor learning. *Neuron, 66*(2), 198–204.

Gandiga, P. C., Hummel, F. C., & Cohen, L. G. (2006). Transcranial DC stimulation (tDCS): a tool for double-blind sham-controlled clinical studies in brain stimulation. *Clinical Neurophysiology, 117*, 845–850.

Gomez Palacio Schjetnan, A., Faraji, J., Metz, G. A., Tatsuno, M., & Luczak, A. (2013). Transcranial direct current stimulation in stroke rehabilitation: a review of recent advancements. *Stroke Research and Treatment*. http://dx.doi.org/10.1155/2013/170256.

Gusnard, D. A., & Raichle, M. E. (2001). Searching for a baseline: functional imaging and the resting human brain. *Nature Reviews Neuroscience, 2*, 685–694.

Huber, R., Maki, H., Rosanova, M., Casarotto, S., Canali, P., Casali, A. G., et al. (2013). Human cortical excitability increases with time awake. *Cerebral Cortex, 23*(2), 332–338.

Ikkai, A., & Curtis, C. E. (2011). Common neural mechanisms supporting spatial working memory, attention and motor intention. *Neuropsychologia, 49*(6), 1428–1434.

Ilmoniemi, R. J., Virtanen, J., Ruohonen, J., Karhu, J., Aronen, H. J., Naatanen, R., et al. (1997). Neuronal responses to magnetic stimulation reveal cortical reactivity and connectivity. *NeuroReport, 8*(16), 3537–3540.

Jacobson, L., Koslowsky, M., & Lavidor, M. (2012). tDCS polarity effects in motor and cognitive domains: a meta-analytical review. *Experimental Brain Research, 216*(1), 1–10.

Kandel, M., Beis, J. M., Le Chapelain, L., Guesdon, H., & Paysant, J. (2012). Non-invasive cerebral stimulation for the upper limb rehabilitation after stroke: a review. *Annals of Physical and Rehabilitation Medicine, 55*(9–10), 657–680.

Keeser, D., Meindl, T., Bor, J., Palm, U., Pogarell, O., Mulert, C., et al. (2011). Prefrontal transcranial direct current stimulation changes connectivity of resting-state networks during fMRI. *The Journal of Neuroscience, 31*(43), 15284–15293.

Keeser, D., Padberg, F., Reisinger, E., Pogarell, O., Kirsch, V., Palm, U., et al. (2011). Prefrontal direct current stimulation modulates resting EEG and event-related potentials in healthy subjects: a standardized low resolution tomography (sLORETA) study. *NeuroImage, 55*(2), 644–657.

Kirimoto, H., Ogata, K., Onishi, H., Oyama, M., Goto, Y., & Tobimatsu, S. (2011). Transcranial direct current stimulation over the motor association cortex induces plastic changes in ipsilateral primary motor and somatosensory cortices. *Clinical Neurophysiology, 122*(4), 777–783.

Lang, N., Siebner, H. R., Ward, N. S., Lee, L., Nitsche, M. A., Paulus, W., et al. (2005). How does transcranial DC stimulation of the primary motor cortex alter regional neuronal activity in the human brain? *The European Journal of Neuroscience, 22*(2), 495–504.

Lehmann, D., & Skrandies, W. (1980). Reference-free identification of components of checkerboard-evoked multichannel potential fields. *Electroencephalography and Clinical Neurophysiology, 48*, 609–621.

Liebetanz, D., Nitsche, M. A., Tergau, F., & Paulus, W. (2002). Pharmacological approach to the mechanisms of transcranial DC-stimulation-induced after-effects of human motor cortex excitability. *Brain, 125*(Pt 10), 2238–2247.

Mancini, F., Bolognini, N., Haggard, P., & Vallar, G. (2012). tDCS modulation of visually induced analgesia. *Journal of Cognitive Neuroscience, 24*(12), 2419–2427.

Massimini, M., Ferrarelli, F., Huber, R., Esser, S. K., Singh, H., & Tononi, G. (2005). Breakdown of cortical effective connectivity during sleep. *Science, 309*(5744), 2228–2232.

Matsunaga, K., Nitsche, M. A., Tsuji, S., & Rothwell, J. C. (2004). Effect of transcranial DC sensorimotor cortex stimulation on somatosensory evoked potentials in humans. *Clinical Neurophysiology, 115*(2), 456–460.

Mattavelli, G., Rosanova, M., Casali, A. G., Papagno, C., & Romero Lauro, L. J. (2013). Top-down interference and cortical responsiveness in face processing: a TMS-EEG study. *NeuroImage, 76*, 24–32.

Miniussi, C., Brignani, D., & Pellicciari, M. C. (2012). Combining transcranial electrical stimulation with electroencephalography: a multimodal approach. *Clinical EEG and Neuroscience, 43*(3), 184–191.

Miniussi, C., & Thut, G. (2010). Combining TMS and EEG offers new prospects in cognitive neuroscience. *Brain Topography, 22*(4), 249–256.

Miranda, P. C., Mekonnen, A., Salvador, R., & Ruffini, G. (2013). The electric field in the cortex during transcranial current stimulation. *NeuroImage, 70*, 48–58.

Monti, A., Ferrucci, R., Fumagalli, M., Mameli, F., Cogiamanian, F., Ardolino, G., & Priori, A. (2013). Transcranial direct current stimulation (tDCS) and language. *Journal of Neurology, Neurosurgery & Psychiatry, 84*(8), 832–842.

Mylius, V., Ayache, S. S., Zouari, H. G., Aoun-Sebaiti, M., Farhat, W. H., & Lefaucheur, J. P. (2012). Stroke rehabilitation using noninvasive cortical stimulation: hemispatial neglect. *Expert Review of Neurotherapeutics, 12*(8), 983–991.

Nitsche, M. A., Boggio, P. S., Fregni, F., & Pascual-Leone, A. (2009). Treatment of depression with transcranial direct current stimulation (tDCS): a review. *Experimental Neurology, 219*(1), 14–19.

Nitsche, M. A., Cohen, L. G., Wassermann, E. M., Priori, A., Lang, N., Antal, A., et al. (2008). Transcranial direct current stimulation: state of the art 2008. *Brain Stimulation, 1*(3), 206–223.

Nitsche, M. A., Fricke, K., Henschke, U., Schlitterlau, A., Liebetanz, D., Lang, N., et al. (2003). Pharmacological modulation of cortical excitability shifts induced by transcranial direct current stimulation in humans. *The Journal of Physiology, 553*(Pt 1), 293–301.

Nitsche, M. A., Grundey, J., Liebetanz, D., Lang, N., Tergau, F., & Paulus, W. (2004). Catecholaminergic consolidation of motor cortical neuroplasticity in humans. *Cerebral Cortex, 14*(11), 1240–1245.

Nitsche, M. A., Jaussi, W., Liebetanz, D., Lang, N., Tergau, F., & Paulus, W. (2004). Consolidation of human motor cortical

neuroplasticity by D-cycloserine. *Neuropsychopharmacology, 29*(8), 1573—1578.

Nitsche, M. A., Liebetanz, D., Antal, A., Lang, N., Tergau, F., & Paulus, W. (2003). Modulation of cortical excitability by weak direct current stimulation—technical, safety and functional aspects. *Supplements to Clinical Neurophysiology, 56*, 255—276.

Nitsche, M. A., & Paulus, W. (2000). Excitability changes induced in the human motor cortex by weak transcranial direct current stimulation. *The Journal of Physiology, 527*(Pt 3), 633—639.

Nitsche, M. A., & Paulus, W. (2001). Sustained excitability elevations induced by transcranial DC motor cortex stimulation in humans. *Neurology, 57*(10), 1899—1901.

Nitsche, M. A., & Paulus, W. (2009). Noninvasive brain stimulation protocols in the treatment of epilepsy: current state and perspectives. *Neurotherapeutics, 6*(2), 244—250.

Nitsche, M. A., & Paulus, W. (2011). Transcranial direct current stimulation—update 2011. *Restorative Neurology and Neuroscience, 29*(6), 463—492.

Nitsche, M. A., Seeber, A., Frommann, K., Klein, C. C., Rochford, C., Nitsche, M. S., et al. (2005). Modulating parameters of excitability during and after transcranial direct current stimulation of the human motor cortex. *The Journal of Physiology, 568*(Pt 1), 291—303.

O'Connell, N. E., Wand, B. M., Marston, L., Spencer, S., & Desouza, L. H. (2011). Non-invasive brain stimulation techniques for chronic pain. A report of a Cochrane systematic review and meta-analysis. *European Journal of Physical and Rehabilitation Medicine, 47*(2), 309—326.

Opitz, A., Windhoff, M., Heidemann, R. M., Turner, R., & Thielscher, A. (2011). How the brain tissue shapes the electric field induced by transcranial magnetic stimulation. *NeuroImage, 58*, 849—859.

Pellicciari, M. C., Brignani, D., & Miniussi, C. (2013). Excitability modulation of the motor system induced by transcranial direct current stimulation: a multimodal approach. *NeuroImage, 83*, 569—580.

Pena-Gomez, C., Sala-Lonch, R., Junque, C., Clemente, I. C., Vidal, D., Bargallo, N., et al. (2012). Modulation of large-scale brain networks by transcranial direct current stimulation evidenced by resting-state functional MRI. *Brain Stimulation, 5*(3), 252—263.

Polania, R., Nitsche, M. A., & Paulus, W. (2011). Modulating functional connectivity patterns and topological functional organization of the human brain with transcranial direct current stimulation. *Human Brain Mapping, 32*(8), 1236—1249.

Polania, R., Paulus, W., Antal, A., & Nitsche, M. A. (2011). Introducing graph theory to track for neuroplastic alterations in the resting human brain: a transcranial direct current stimulation study. *NeuroImage, 54*(3), 2287—2296.

Poreisz, C., Boros, K., Antal, A., & Paulus, W. (2007). Safety aspects of transcranial direct current stimulation concerning healthy subjects and patients. *Brain Research Bulletin, 72*(4—6), 208—214.

Priori, A., Berardelli, A., Rona, S., Accornero, N., & Manfredi, M. (1998). Polarization of the human motor cortex through the scalp. *NeuroReport, 9*(10), 2257—2260.

Purpura, D. P., & McMurtry, J. G. (1965). Intracellular activities and evoked potential changes during polarization of motor cortex. *Journal of Neurophysiology, 28*, 166—185.

Rossi, S., Hallett, M., Rossini, P. M., Pascual-Leone, A., &, The Safety of TMS Consensus Group. (2009). Safety, ethical considerations, and application guidelines for the use of transcranial magnetic stimulation in clinical practice and research. *Clinical Neurophysiology, 120*, 2008—2039.

Schestatsky, P., Morales-Quezada, L., & Fregni, F. (2013). Simultaneous EEG monitoring during transcranial direct current stimulation. *Journal of Visualized Experiments*, (76).

Shomstein, S. (2012). Cognitive functions of the posterior parietal cortex: top-down and bottom-up attentional control. *Frontiers in Integrative Neuroscience, 6*, 38.

Sparing, R., Thimm, M., Hesse, M. D., Küst, J., Karbe, H., & Fink, G. R. (2009). Bidirectional alterations of interhemispheric parietal balance by non-invasive cortical stimulation. *Brain, 132*(11), 3011—3020.

Stagg, C. J., Best, J. G., Stephenson, M. C., O'Shea, J., Wylezinska, M., Kincses, Z. T., et al. (2009). Polarity-sensitive modulation of cortical neurotransmitters by transcranial stimulation. *The Journal of Neuroscience, 29*(16), 5202—5206.

Stagg, C. J., Lin, R. L., Mezue, M., Segerdahl, A., Kong, Y., Xie, J., et al. (2013). Widespread modulation of cerebral perfusion induced during and after transcranial direct current stimulation applied to the left dorsolateral prefrontal cortex. *The Journal of Neuroscience, 33*(28), 11425—11431.

Stone, D. B., & Tesche, C. D. (2009). Transcranial direct current stimulation modulates shifts in global/local attention. *NeuroReport, 20*(12), 1115—1119.

Utz, K. S., Dimova, V., Oppenlander, K., & Kerkhoff, G. (2010). Electrified minds: transcranial direct current stimulation (tDCS) and galvanic vestibular stimulation (GVS) as methods of non-invasive brain stimulation in neuropsychology — a review of current data and future implications. *Neuropsychologia, 48*(10), 2789—2810.

Vallar, G., & Bolognini, N. (2011). Behavioural facilitation following brain stimulation: implications for neurorehabilitation. *Neuropsychological Rehabilitation, 21*(5), 618—649.

Virtanen, J., Ruohonen, J., Naatanen, R., & Ilmoniemi, R. J. (1999). Instrumentation for the measurement of electric brain responses to transcranial magnetic stimulation. *Medical and Biological Engineering and Computing, 37*(3), 322—326.

Windhoff, M., Opitz, A., & Thielscher, A. (2013). Electric field calculations in brain stimulation based on finite elements: an optimized processing pipeline for the generation and usage of accurate individual head models. *Human Brain Mapping, 34*, 923—935.

Wirth, M., Rahman, R. A., Kuenecke, J., Koenig, T., Horn, H., Sommer, W., et al. (2011). Effects of transcranial direct current stimulation (tDCS) on behaviour and electrophysiology of language production. *Neuropsychologia, 49*(14), 3989—3998.

Zaehle, T., Beretta, M., Jancke, L., Herrmann, C. S., & Sandmann, P. (2011). Excitability changes induced in the human auditory cortex by transcranial direct current stimulation: direct electrophysiological evidence. *Experimental Brain Research, 215*(2), 135—140.

Zheng, X., Alsop, D. C., & Schlaug, G. (2011). Effects of transcranial direct current stimulation (tDCS) on human regional cerebral blood flow. *NeuroImage, 58*(1), 26—33.